

# Percolation on the square lattice in a $L \times M$ geometry

## Analysis of percolation clusters properties

R.A. Monetti, E.V. Albano

Instituto de Investigaciones Fisicoquímicas Teóricas y Aplicadas (INIFTA), Facultad de Ciencias Exactas, Universidad Nacional de La Plata, Sucursal 4, Casilla de Correo 16, 1900 La Plata, Argentina

Received: 5 May 1992 / Revised version: 9 September 1992

**Abstract.** A study of the site percolation model on the square lattice in a  $L \times M$  geometry at critically is presented. For  $L \ll M$  one observes the growth of numerous percolation clusters in the  $L$ -direction in contrast to the absence of percolation in the  $M$ -direction. Consequently, relevant properties of these clusters such as for example the average number of clusters ( $N_{CL}$ ), the cluster length distribution ( $P(l, L)$ , with  $l$ =cluster length in the  $M$  direction) and average cluster length ( $l_{CL}$ ), are studied by means of the Monte Carlo technique and analyzed on the basis of finite-size scaling arguments. The following behavior is found:  $N_{CL} \cong (3/8) (L/M)^{-\delta}$ , with  $\delta=1$ ; and  $l_{CL} \cong 2.0 L$ . Also the distribution  $P(l, L)$  is of the exponential-exponential type and their characteristic exponents are evaluated.

### I. Introduction

Percolation processes are being studied with increasing interest due to their useful applications in many fields of physics and physical-chemistry. There is now a vast literature on the subject such as, for example, the reviews [1–6] and references therein. Remarkably, most of the available work on percolation in two dimensions, performed using different techniques, has been done in a  $L \times L$  geometry [1–6]. Nevertheless, also numerous authors have considered non-quadratic shapes in percolation theory. In fact,  $L \times M$  and strip geometries have been studied by means of transfer matrix and phenomenological renormalization methods, see for example [7–11] and references therein. Furthermore, studies of other models in rectangular or strip geometries, such as for example the Ising model ([12–14] and references therein), have demonstrated that this is an useful approach which contribute to the understanding of the whole problem. In a recent work [15] we have analyzed some aspects of the critical behavior of the site percolation model on

the square lattice in a  $L \times M$  geometry. This geometry is particularly suitable for the study of adsorption phenomena at stepped surfaces [12–16] as well as for diffusion and conduction processes in layered media [6].

A remarkable feature of the percolation process under the constraint  $L \ll M$  is the preferential development of percolating clusters in the  $L$ -direction of the lattice (see for example Fig. 2 of [15]). In fact, one has that for a relatively small site occupation probability ( $p=0.5$ ) percolating clusters in the  $L$ -direction have already grown. Right at the critical threshold  $p=p_c \cong 0.59275$  one observes numerous percolation clusters along the  $L$ -direction. The development of a percolating cluster in the  $M$ -direction can hardly occur for  $L \ll M$  at  $p_c$  but it is frequently observed for  $p=0.70 \gg p_c$  [15].

Based upon these considerations, the aim of the present work is to study, at critically, some relevant properties of the percolation clusters in the  $L$ -direction and their dependence on the aspect ratio ( $L/M$ ) of the sample. Within this context the average number of percolating clusters, the average cluster length and the cluster-length-distribution, are evaluated by means of Monte Carlo simulations and discussed on the basis of finite size scaling arguments. It should be emphasized that the study of the above mentioned properties has not been addressed yet. Let us also note that the study of the appropriate distributions gives valuable information on structural cluster properties ([17] and references therein) and consequently is a subject of considerable interest. For example, probability distributions for several fractal properties such as the voltage distribution in percolation and the growth probabilities of diffusion-limited aggregation have been found to be of log-normal type [18–20]. Also the distribution of mass within a certain radius has been evaluated for percolation clusters generated on a Cayley tree and diffusion-limited aggregates [21, 22]. In most cases, an infinite hierarchy of independent exponents is needed to characterize the different moments, so multifractal behavior is found.

## II. Results and discussion

Details on the site percolation model have already been published in various reviews [1–6], so they do not need to be repeated here. In the present work, the Monte Carlo simulations are performed using free boundary conditions in both  $L$  and  $M$ -directions, clusters are identified using standard algorithms and results are typically averaged over  $10^3$ – $10^5$  different configurations, depending on the lattice size, in order to achieve reasonable statistics [15].

### II.a. The average number of percolating clusters at $p_c$

As it has been already discussed, right at  $p_c$  there are few percolating clusters in the  $L$ -direction, but not in the  $M$ -direction, due to the fact that  $L \ll M$ . In order to analyze the average number of percolating clusters in the  $L$ -direction  $\langle N_{CL} \rangle$  at critically, let us make two simple considerations:

i) Since in two dimensions right at  $p_c$  there exist a single percolating cluster the behavior  $\langle N_{CL} \rangle \rightarrow 1$  for  $L, M \rightarrow \infty, p = p_c$  is expected to hold. This behavior should also hold for  $L \simeq M$ .

ii) Keeping  $L = \text{constant}$  and  $M \rightarrow \infty$  one expects  $\langle N_{CL} \rangle \rightarrow \infty$ .

So, under assumptions i) and ii) it is natural to suggest the following power law approach

$$\langle N_{CL} \rangle \propto (L/M)^{-\delta}, \quad L \ll M, \quad (1)$$

where  $\delta > 0$  is an exponent which has to be determined. Figure 1 shows a log-log plot of  $\langle N_{CL} \rangle$  versus  $L/M$  for samples of different sizes. The plot shows a reasonable data collapsing into a straight line with slope  $\delta = 1$ . Nevertheless, a careful inspection of Fig. 1 reveals systematic deviation of the data for fixed values of  $L/M$ . Similar deviations appear analyzing the probability of a site belonging to the biggest cluster and can be understood as due to scaling corrections of the order  $L^{-1}$  to the leading term [15].

According to assumption ii) and the fact that  $\delta = 1$ ,  $\langle N_{CL} \rangle$  should increase linearly with  $M$  for constant values of the sample width  $L$ . Figure 2 shows that the expected behavior holds because data points define straight lines with different slopes ( $S_1(L)$ ) for fixed values of  $L$ . A plot of  $S_1(L)$  vs.  $L^{-\delta}$ , as it is suggested by (1), gives a straight line (Fig. 3) with slope  $C_1 \cong 3/8$ . So, from Figs. 1–3 and the above discussion, it follows that

$$\langle N_{CL} \rangle = S_1(L) M \cong (3/8)(L/M)^{-\delta}, \quad \delta = 1, \quad L \ll M. \quad (2)$$

This result will be further discussed below.

### II.b. The average length of the percolating clusters at $p_c$

The growth of percolating clusters in the  $L$ -direction, due to the constraint  $L \ll M$ , can be qualitatively compared with the development of domains of spins-up and

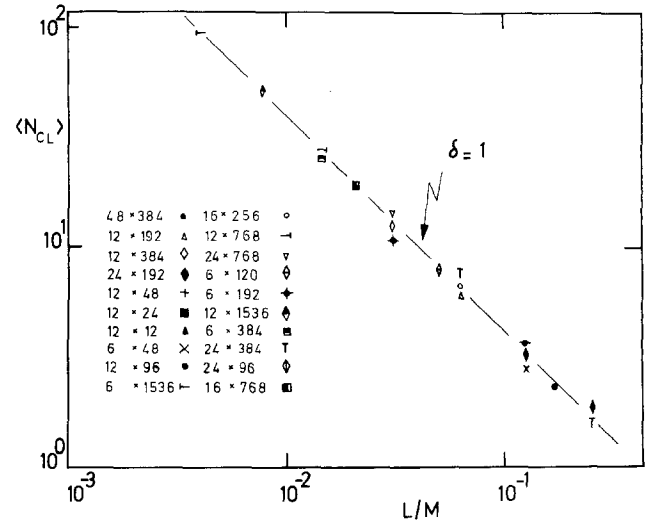


Fig. 1. Log-log plot of the average number of percolating clusters  $\langle N_{CL} \rangle$  at  $p_c$  versus  $L/M$  for samples of different size as indicated by the symbols. The straight line with slope  $\delta = 1$  has been drawn for comparison. More details in the text

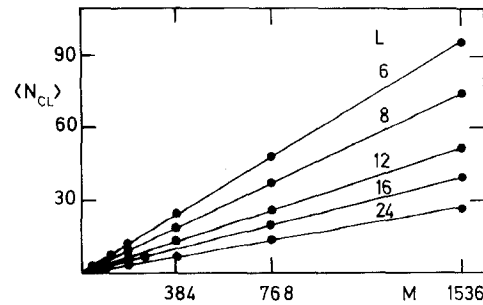


Fig. 2. Plot of  $\langle N_{CL} \rangle$  at  $p_c$  versus  $M$  for samples of different width  $L$

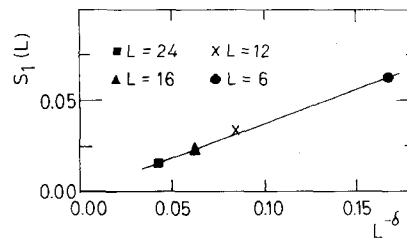


Fig. 3. Plot of the slope  $S_1(L)$ , as determined from Fig. 2, versus  $L^{-\delta}$  with  $\delta = 1$ . Individual choices of the lattice width  $L$  are indicated by different symbols. The straight line with slope  $C_1 = 3/8$  has been drawn for comparison

spins-down crossing through the sample ( $L$ -direction), observed for the same geometry, working with the ferromagnetic Ising model in absence of both bulk and surface fields [12–14]. From conformal invariance [23] and Monte Carlo results [12, 13] it follows that the average distance  $\langle l_d \rangle$  between the border of domains with different spins is given by  $\langle l_d \rangle = (\pi/2)^{-1} L$ . Similarly, for the percolation process at  $p_c$  in the  $L \times M$  geometry one can define the average length  $\langle l_{CL} \rangle$  (along the  $M$ -direction) of percolating clusters in the  $L$ -direction. Now, let us

show that  $\langle l_{CL} \rangle$  should be of the order of  $L$ . It is known from finite-size scaling arguments that the average probability of a site belonging to the largest (percolating) cluster  $P_a(L, M)$  behaves like [15]

$$P_a(L, M) = L^{-\beta/\nu} F(L/M, (p - p_c) L^{1/\nu}), \quad (3)$$

where  $\beta = 5/36$ ,  $\nu = 4/3$ ,  $F$  is a suitable scaling function and the subindex  $a$  stress the fact that we are referring to the average probability taken over all those clusters percolating in the  $L$ -direction. Note that right at  $p_c$  the second scaling variable vanishes. So, assuming the average mass ( $m(p = p_c)$ ) of the cluster is given by

$$m(p = p_c) \propto P_a(L, M) \langle l_{CL} \rangle L, \quad (4a)$$

and it behaves like [3–6]

$$m(p = p_c) \propto L^{D_F}, \quad D_F = d - \beta/\nu, \quad (4b)$$

and taking into account that  $F(L/M, 0) \simeq (L/M)$  [15] it follows that

$$\langle l_{CL} \rangle \propto L, \quad L/M = \text{constant}. \quad (5)$$

That is, the finite-size scaling analysis gives the same power dependence of  $\langle l_{CL} \rangle$  on  $L$  than conformal invariance applied to the Ising model ( $\langle l_D \rangle$ , see above), but in contrast the proportionality constant is not fixed at all by scaling arguments. Equation (5) can also be obtain in a somewhat more qualitative manner. In fact, it is natural to assume that

$$\langle N_{CL} \rangle \langle l_{CL} \rangle \simeq M \quad (6)$$

and using (1) with  $\delta = 1$  one recovers (5). Figure 4 shows a plot of  $\langle l_{CL} \rangle$  versus  $M$  for lattices of different aspect ratio,  $0.015625 \leq L/M \leq 0.5$ . It is found that the data points nicely define straight lines only for fixed values of  $L/M$  and that the slopes of such lines  $\{S_2(L/M)\}$  also

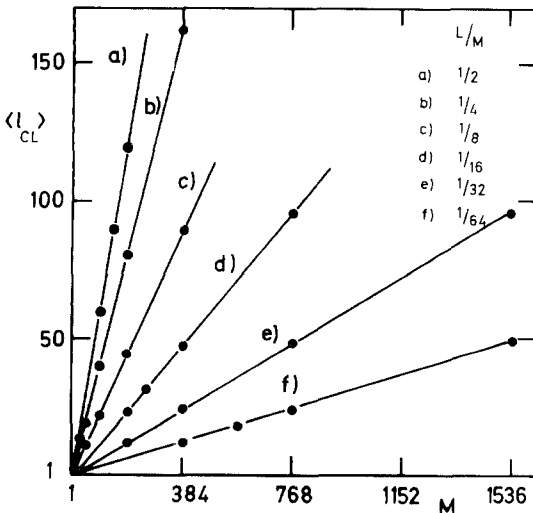


Fig. 4. Plot of the average cluster width  $\langle l_{CL} \rangle$  at  $p_c$  versus  $M$  for samples of different aspect ratio  $L/M$  as indicated by the symbols. The straight lines are obtained by least square fits of the data points

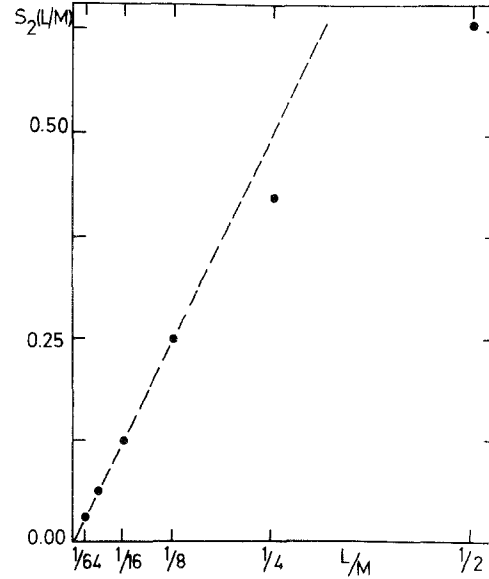


Fig. 5. Plot of the slope  $S_2(L/M)$ , as determined from Fig. 4, versus the aspect ratio  $L/M$ . The straight line with slope  $C_2 = 2$  is obtained in the limit  $L \ll M$

depend on  $L/M$ , that is

$$\langle l_{CL} \rangle = S_2(L/M) M. \quad (7)$$

A plot of  $S_2(L/M)$ , versus  $L/M$  is shown in Fig. 5. It is interesting to note that, in the limit  $L \ll M$ , Fig. 5 suggests that the following behavior should hold

$$S_2(L/M) = C_2 L/M, \quad C_2 \simeq 2.0. \quad (8)$$

Therefore, using (7) and (8) it follows

$$\langle l_{CL} \rangle \simeq 2.0 L, \quad L \ll M, \quad (9)$$

in agreement with the scaling result and the qualitative estimation (5) but the proportionality constant has now been determined with the aid of the Monte Carlo data. Note that deviation from the straight line behavior observed in Fig. 5 for  $L/M = 1/4$  and  $1/2$  are due to the fact that for these cases one has severe restrictions to the growth of clusters with length larger than  $\langle l_{CL} \rangle$  or even than  $L$ . Coming back to our comparison with results of the ferromagnetic Ising model [12] one has that  $\langle l_d \rangle < L$  in contrast to  $\langle l_{CL} \rangle > L$ .

Summing up, Monte Carlo data suggest that in the asymptotic regime  $M \gg L$  the average cluster length does not depend on the aspect ratio but is a function of  $L$  only. A plot of  $\langle l_{CL} \rangle / 2L$  vs.  $M$  (Fig. 6) shows that the above statement holds and that for  $M \gg L$  the average cluster length tends to a saturation value close to  $2L$  in agreement with (9). Nevertheless, a careful inspection of Fig. 6 reveals that, for  $L \ll M$ , data points are not uniformly scattered around the straight line given by  $\langle l_{CL} \rangle / 2L = 1$ , as it should be caused by statistical fluctuations characteristics of the Monte Carlo results. In fact, most points lie above than the expected value suggesting either that  $C_2$  should be slightly greater than 2 or that scaling corrections to the leading term would be neces-

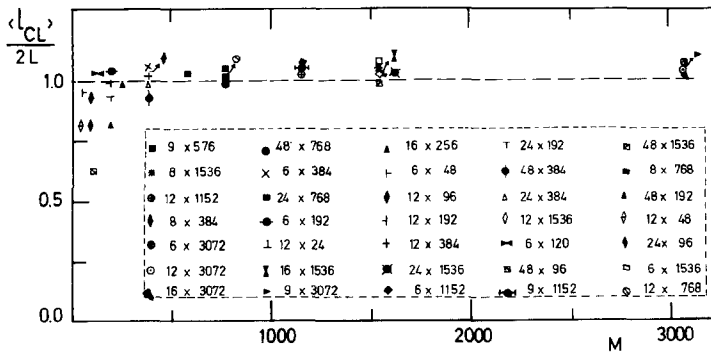


Fig. 6. Plot of  $\langle l_{CL} \rangle / 2L$  versus  $M$  for different choices of the lattice size as indicated by the symbols. The dashed straight line given by  $\langle l_{CL} \rangle / 2L = 1$  has been drawn for comparison. More details in the text

sary. Regrettably, we are not able to elucidate the actual reason because it requires the study of large lattices with huge statistics and consequently prohibitive computing time.

II.c. The cluster length distribution at  $p_c$

This section is devoted to the discussion of the cluster length distribution  $P(l, L)$ , defined as the probability to have a cluster of length  $l$  in a sample of width  $L$ , assuming  $L \ll M$ . Notice that all clusters have to be percolating clusters in the  $L$ -direction and consequently the cluster length is measured in the perpendicular  $M$ -direction. Also note that in the limit  $L \ll M$  the dependence of  $P(l, L)$  on  $M$  can be neglected. Figure 7 shows log-log plots of  $P(l, L)$  versus  $l$  for samples of different size. An inspection of Fig. 7 reveals that the curves are not symmetric around the maximum and that the magnitude of such maxima decreases when increasing  $L$ , irrespective of the sample length. In order to understand the above mentioned dependence it is convenient to analyze the scaling behavior of  $P(l, L)$ . So, let us first evaluate the average cluster length  $\langle l_{CL} \rangle$ , already discussed in Sect. II.b. Using the distribution function one has

$$\langle l_{CL} \rangle = \sum l P(l, L). \tag{10}$$

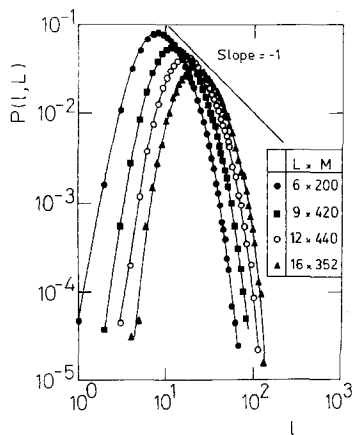


Fig. 7. Log-log plot of the cluster length distribution  $P(l, L)$  versus  $l$  for different choices of the lattice size as indicated by the symbols. The straight line with slope  $-1$  has been drawn in order to show the behavior of the distribution maximum. More details in the text

Now we assume that at critically  $P(l, L)$  is an homogeneous function, so

$$P(l, L) = L^{-\omega} f(l/L) \tag{11}$$

where  $\omega$  is an exponent and  $f$  is a suitable scaling function. Inserting (11) into (10) and integrating the summation using standard techniques [3] it follows

$$\langle l_{CL} \rangle = \int dl l L^{-\omega} f(l/L) = L^{2-\omega} \int u f(u) du, \tag{12}$$

where  $u = l/L$  and consequently

$$\langle l_{CL} \rangle \propto L^{2-\omega}. \tag{13}$$

But according to (5) or (9) one has that  $\langle l_{CL} \rangle \propto L^1$ , so comparing to (13) it follows  $\omega = 1$ . Before checking the validity of the above statement it is convenient to analyze the dependence on  $L$  of the abscissa of the maxima exhibited by  $P(l, L)$ , say  $l_m$ . Figure 8 shows that a plot of  $l_m$  versus  $L$ , for lattices of different size, exhibits a straight line behavior with slope close to  $4/3$ , so from our Monte Carlo data it follows that

$$l_m \cong 4/3 L, \quad L \ll M. \tag{14}$$

Deviations from the straight line behavior in Fig. 8 observed for the biggest lattice is presumably due to the lack of appropriate statistic. Now, replacing (14) in (11) one has

$$P(l_m, L) = L^{-\omega} f(l_m/L) \cong L^{-\omega} f(4/3) \tag{15}$$

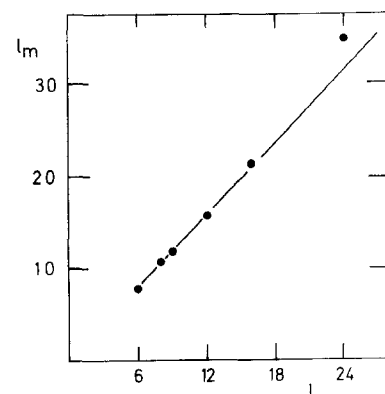
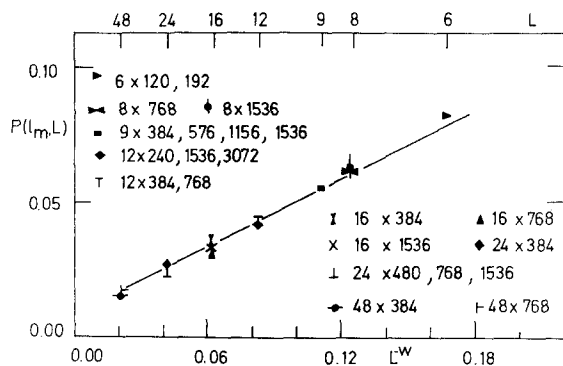


Fig. 8. Plot of  $l_m$  versus  $L$  for various choices of the lattice size. The straight line with slope  $4/3$  has been drawn for comparison



**Fig. 9.** Plot of  $P(l_m, L)$  versus  $L^{-\omega}$  ( $\omega=1$ ) for different choices of the lattice size as specified by the symbols. Note that for certain values of  $L$ , differences due to changes on the lattice length  $M$  are smaller than the size of the points itself. The straight line has slope  $1/2$  and has been drawn for comparison

that is the magnitude of the maxima of  $P(l, L)$  should decay as  $L^{-\omega}$  ( $\omega=1$ ). Figure 9 shows a plot of  $P(l_m, L)$  versus  $L^{-\omega}$  for lattices of different size. The obtained straight line confirms the validity of the scaling hypothesis (11) with  $\omega=1$ . From the slope of Fig. 9 one can also evaluate the scaling function for a particular value of its argument, i.e.  $f(4/3) \cong 1/2$ . Pointing now again our attention to Fig. 7, the straight line with slope  $=-1$  can also be used to check the  $L^{-\omega}$  dependence of  $P(l_m, L)$  by virtue of the linear relationship given by (14).

A more conclusive test of the scaling hypothesis involved in (11) is shown in Fig. 10 where  $P(l, L)/P(l_m, L)$  is plotted against  $l/L$  for samples of different size. The excellent data collapsing observed strongly supports the validity of (11). Also, the shape of the collapsed curve suggests that the distribution function may be of the exp-exp type, i.e.

$$P(l, L) L^\omega = \exp[A + B(l/L)^{-\Delta_1} + C(l/L)^{\Delta_2}] \quad (16)$$

where  $A$ ,  $B$  and  $C$  are constants and  $\Delta_1$  and  $\Delta_2$  are the characteristic exponents. A least squared regression of the data points gives for the best fit (shown by a

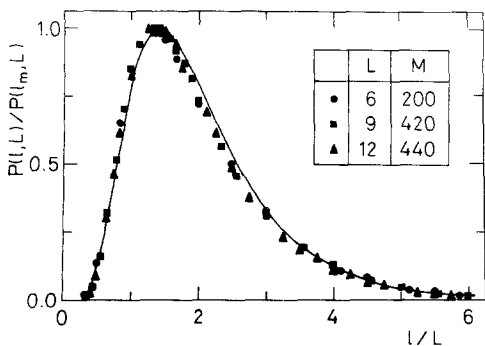


**Fig. 10.** Plot of the cluster length distribution normalized with respect to its maximum versus  $l/L$  for lattices of different size. The full line corresponds to the best fit obtained with the exp-exp distribution given by (16) using the constants and exponents listed in (17)

solid line in Fig. 10) the following result:

$$A \cong 84.9, \quad B \cong -46.6, \\ C \cong -38.6 \quad \text{and} \quad \Delta_1 \cong \Delta_2 \cong 0.21. \quad (17)$$

It is interesting to note that, at critically, the distribution of mass within the topological distance for percolation clusters generated in both, Cayley trees [21] and the square lattice [17], also exhibits an exp-exp behavior.

### III. Concluding remarks

Relevant properties of percolating clusters of the site percolation model in the  $L \times M$  ( $L \ll M$ ) geometry at critically have been studied by means of Monte Carlo simulations and a finite-size scaling analysis. In order to gain further insight on the subject, a study of the correlation function behavior is under progress.

This work is financially supported by the Consejo Nacional de Investigaciones Científicas y Técnicas (CONICET) de la República Argentina. R.A.M. gratefully acknowledge the Comisión de Investigaciones Científicas (CIC) de la Provincia de Buenos Aires (Argentina) for the provision of a fellowship. E.V.A. would like to acknowledge stimulating discussions with Profs. K. Binder and D. Heermann.

### References

1. Stauffer, D.: Phys. Rep. **54**, 1 (1979)
2. Stauffer, D., Coniglio, A., Adam, A.: Avd. Polymer Sci. **44**, 103 (1982)
3. Stauffer, D.: In: Introduction to percolation theory. London: Taylor and Francis 1985
4. Heermann, H.: Phys. Rep. **136**, 143 (1986)
5. Aharony, A.: In: Percolation. Grinstein, G., Mazenko, G. (eds.). Singapore: World Scientific 1986
6. Feders, J.: In: Fractals. New York: Plenum Press 1988
7. Derrida, B., Vannimemus, J.: J. Phys. (Paris) **41**, L473 (1980)
8. Derrida, B., De Seze, L.: J. Phys. (Paris) **43**, 475 (1982)
9. Nightingale, P.: J. Appl. Phys. **53**, 7927 (1982)
10. Normand, J.M., Heermann, H.J., Hajjar, M.: J. Stat. Phys. **52**, 441 (1988)
11. Lam, P.M.: J. Stat. Phys. **54**, 1081 (1989)
12. Albano, E.V., Binder, K., Heermann, D.W., Paul, W.: Z. Phys. B - Condensed Matter **77**, 445 (1989)
13. Albano, E.V., Binder, K., Heermann, D.W., Paul, W.: Surf. Sci. **223**, 151 (1989)
14. Albano, E.V., Binder, K., Heermann, D.W., Paul, W.: J. Chem. Phys. **91**, 3700 (1989)
15. Monetti, R.A., Albano, E.V.: Z. Phys. B - Condensed Matter **82**, 129 (1991)
16. Wagner, H.: In: Physical and chemical properties of stepped surfaces. Springer Tracts in Modern Physics. Vol. 85, Höhler, G. (ed.). Berlin, Heidelberg, New York: Springer 1979
17. Neumann, A.U., Havlin, S.: J. Stat. Phys. **52**, 203 (1988)
18. de Arcangelis, L., Redner, S., Coniglio, A.: Phys. Rev. B **31**, 4725 (1986); **34**, 4656 (1986)
19. Halsey, T.L., Meakin, P., Procaccia, I.: Phys. Rev. Lett. **56**, 854 (1986)
20. Amitrano, C., Coniglio, A., di Liberto, F.: Phys. Rev. Lett. **57**, 1016 (1986)
21. Havlin, S., Kiefer, J., Leyvraz, F., Weiss, G.H.: J. Stat. Phys. **47**, 173 (1987)
22. Meakin, P., Havlin, S.: Phys. Rev. A **36**, 4428 (1987)
23. Cardy, J.L.: J. Phys. A **17**, L385 (1984) and In: Phase transitions and critical phenomena. Domb, C., Lebowitz, J.L. (eds.), Vol. XI, p. 84. New York: Academic Press 1987